



**HAL**  
open science

# Tracking fluids in multiple scattering and highly porous materials: toward applications in non-destructive testing and seismic monitoring

Romain Théry, Antoine Guillemot, Odile Abraham, Éric Larose

## ► To cite this version:

Romain Théry, Antoine Guillemot, Odile Abraham, Éric Larose. Tracking fluids in multiple scattering and highly porous materials: toward applications in non-destructive testing and seismic monitoring. *Ultrasonics*, 2020, 102, pp.106019. 10.1016/j.ultras.2019.106019 . hal-02376463

**HAL Id: hal-02376463**

**<https://hal.science/hal-02376463>**

Submitted on 22 Nov 2019

**HAL** is a multi-disciplinary open access archive for the deposit and dissemination of scientific research documents, whether they are published or not. The documents may come from teaching and research institutions in France or abroad, or from public or private research centers.

L'archive ouverte pluridisciplinaire **HAL**, est destinée au dépôt et à la diffusion de documents scientifiques de niveau recherche, publiés ou non, émanant des établissements d'enseignement et de recherche français ou étrangers, des laboratoires publics ou privés.

1 Tracking fluids in multiple scattering and highly porous  
2 materials: toward applications in non-destructive testing and  
3 seismic monitoring

4 Romain Théry\*<sup>1</sup>, Antoine Guillemot<sup>2</sup>, Odile Abraham<sup>1</sup>, and Éric Larose<sup>2</sup>

5 <sup>1</sup>*IFSTTAR-GERS, Laboratoire Géophysique et Évaluation Non Destructive, Bouguenais, France*

6 <sup>2</sup>*Univ. Grenoble Alpes, CNRS - ISTerre - Grenoble, France*

7 **Abstract**

8 Seismic and ultrasonic waves are sometimes used to track fluid injections, propagation,  
9 infiltrations in complex material, including geological and civil engineered ones. In most  
10 cases, one use the acoustic velocity changes as a proxy for water content evolution. Here we  
11 propose to test an alternative seismic or acoustic observable : the waveform decorrelation.

12 We use a sample of compacted millimetric sand as a model medium of highly porous multiple  
13 scattering materials. We fill iteratively the sample with water, and track changes in ultrasonic  
14 waveforms acquired for each water level. We take advantage of the high sensitivity of diffuse  
15 coda waves (late arrivals) to track small water elevation in the material. We demonstrate  
16 that in the mesoscopic regime where the wavelength, the grain size and the porosity are in the  
17 same order of magnitude, Coda Wave Decorrelation (waveform change) is more sensitive to  
18 fluid injection than Coda Wave Interferometry (apparent velocity change). This observation  
19 is crucial to interpret fluid infiltration in concrete with ultrasonic record changes, as well as  
20 fluid injection in volcanoes or snow melt infiltration in rocky glaciers. In these applications,  
21 Coda Wave Decorrelation might be an extremely interesting tool for damage assessment and  
22 alert systems.

23 **Keywords:** porous media, multiple scattering, coda, fluid migration

24 **1 Introduction**

25 Tracking fluids in porous media is a common problematic to several fields of research, from geol-  
26 ogy (hydro-geology, oil prospection, CO<sub>2</sub> sequestration, volcanology) to civil engineering (struc-

---

\*romain.thery@ifsttar.fr

27 tural health monitoring and non destructive evaluation). The goals of these researches are usually  
28 to detect, locate and quantify fluid flows. In practice, electrical and electromagnetic techniques  
29 have been largely used [Archie, 1942, Benson, 1991, Barker & Moore, 1998, Villain et al., 2012].  
30 Remote and light, these techniques yet encounter limits, for instance in presence of conduc-  
31 tive materials (such as clay or metals). The many success of elastic waves in imagery, along  
32 with their relative simplicity of implementation, suggest mechanical waves as a relevant alterna-  
33 tive. Elastic waves are indeed very sensitive to the mechanical properties of their propagation  
34 medium. Numerous papers have been published, investigating water content effects on elastic  
35 waves propagation, in various porous medium. Among them, field studies on sedimentary soils  
36 [Konstantaki et al., 2013], laboratory experiments on rocks [Winkler & Nur, 1979] or concrete  
37 [Abraham et al., 2012, Garnier et al., 2013], which all show variations of elastic waves veloci-  
38 ties and attenuation with water content. These variations aren't always monotonic, and differ  
39 according to the type of media. However, these studies consider ballistic wave propagation.  
40 Indeed, wavelength are significantly larger than pore or grain size.

41 In this paper we use multiply scattered waves, with wavelength smaller or equal to the  
42 pore size, in order to detect changes induced by fluid infiltrating in porous media. These  
43 waves, also named coda-waves, spend a larger amount of time propagating through the medium,  
44 and hence interact more with changes. This high sensitivity of coda waves has been proven  
45 [Snieder et al., 2002] and used in many applications, from volcanoes and fault zones moni-  
46 toring [Sens-Schönfelder & Wegler, 2006, Brenguier et al., 2008] to crack detection in concrete  
47 [Zhang et al., 2012, Zhang et al., 2016, Zhang et al., 2018]. Coda Wave interferometry (CWI)  
48 is a coda-based technique permitting to extract an apparent velocity change in the media,  
49 whereas Coda Wave Decorrelation (CWD) allows to assess and quantify structural or geomet-  
50 rical changes. [Grêt et al., 2006] already showed that CWI is sensitive to fluid presence in  
51 sandstone. We here present the results of an experiment aiming to track an increasing water  
52 front in concrete, using CWI and CWD. We then use these results to interpret those from a  
53 similar experiment in concrete, along with observations made on volcanoes and rocky glacier.

## 54 **2 Monitoring of water level elevation in sand**

55 We here present a laboratory experiment aiming at seeing the effects of a water front, ascend-  
56 ing in a compacted and pre-humidified sample of sand, on ultrasonic coda waves emitted and  
57 recorded beneath its surface. We show in Fig. 1 the experimental setup. Millimetric bioclastic  
58 limestone sand is humidified, placed in a cylindrical (13 cm in diameter) glass container, and

59 compacted. The final height of the sample is about 8 cm. The pre-humidification part allows  
 60 us to only consider water saturation - or water content - variations as the causes of change in  
 61 wave propagation. It is indeed known that for weak water saturation values, the impact of water  
 62 potential - or capillary effects - on wave propagation is as important as the one of water content  
 63 [Lu & Sabatier, 2009]. A simple set-up makes it possible to introduce water in the bottom of of  
 64 the container. Water is iteratively added and its height is visually controlled through the glass  
 65 wall.

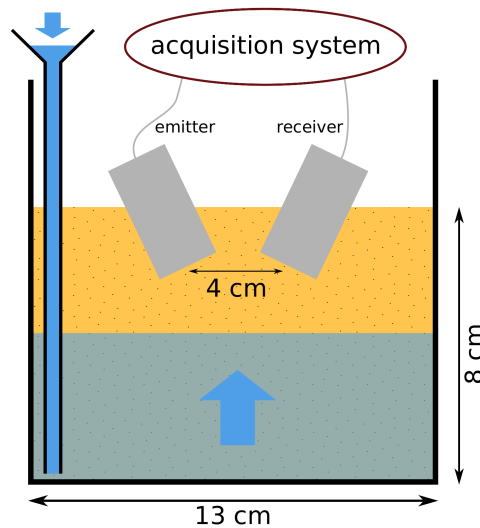


Figure 1: Set-up of the experiment.

A water front ascending in a pre-humidified and compacted sand sample is monitored using ultrasonic coda.

66 Two ultrasonic transducers used in the emitter-receiver configuration, are buried 2 cm below  
 67 the surface of the sample. Impulse responses are retrieved for each incremental water level step,  
 68 by correlating the measured signal (averaged over 200 acquisitions) with the source signal (linear  
 69 chirp from 200 kHz to 400 kHz).

70 Acquired impulse responses (Fig. 2) show no distinct first arrival. Indeed in our experiment,  
 71 the grain size  $S$  is ranging from 0.1 mm to 2 mm, and the wavelength  $\lambda$  is of the order of  
 72 a few millimeters. According to literature [Jia, 2004, Jia et al., 2009] we can estimate the  
 73 scattering mean free path  $l^*$  to be ranging from approximately a few millimeters to a few  
 74 centimeters. Furthermore, the size of the medium  $H$  is 12 cm (twice the distance separating the  
 75 sensors from the bottom of the container). Thus we are in the multiple scattering regime, where  
 76  $S < \lambda < l^* < H$ .

77 Although coda's complex waveform could be interpreted as noise, it is in fact a deterministic  
 78 and reproducible signal. Furthermore, coda waves spend more time than ballistic ones in the  
 79 medium, hence interacting more often with possible developing changes. This high sensitivity

80 of coda waves, along with their reproducibility, have led to the development of Coda Wave  
 81 Interferometry techniques [Snieder et al., 2002, Snieder, 2006].

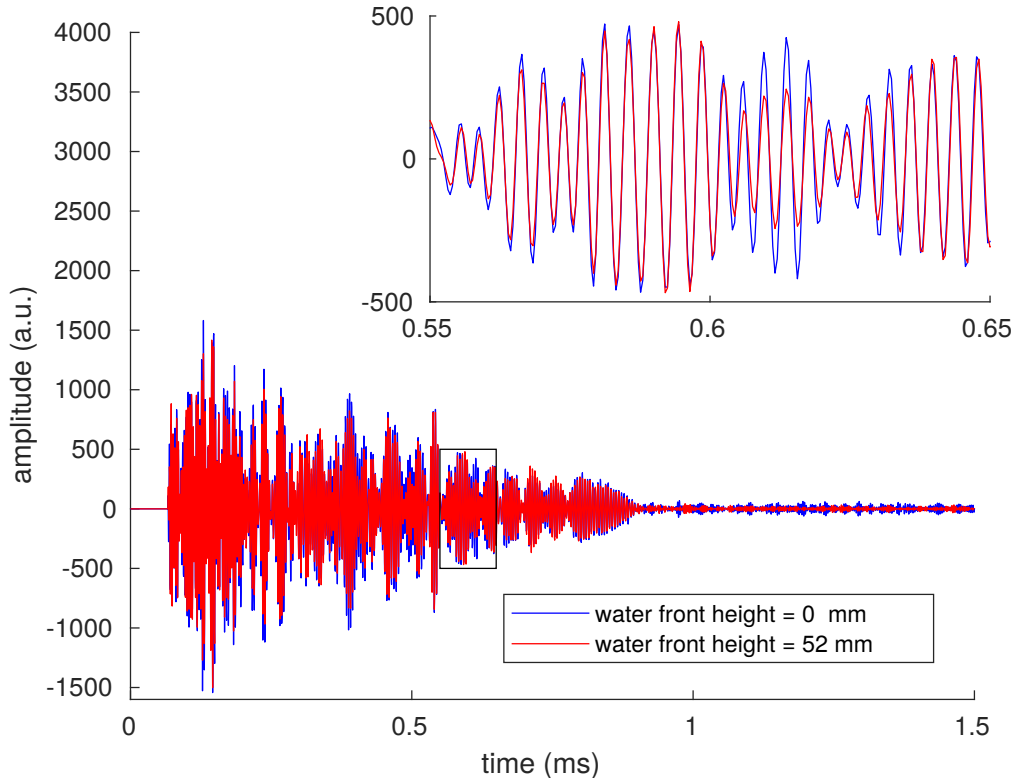


Figure 2: Impulse responses measured before and during imbibition. First amplitude values of the signals have been manually set to zero, in order to mask a single peak corresponding to cross-talk in the recordings. This modification only aims to simplify the figure without any consequences on our results, since early arrivals aren't studied here. Inset shows a close-up around the center of the observation time window used in the following. Although waveforms are different, phase shifts are hardly visible.

82 We then compare each impulse response with the reference one (recorded before addition of  
 83 water). Hence using the reproducibility property of coda waves, we apply the stretching tech-  
 84 nique [Lobkis & Weaver, 2003, Sens-Schönfelder & Wegler, 2006, Larose & Hall, 2009] to track  
 85 phase and waveform changes in the signal, with increasing water level. Let us consider the  
 86 reference signal, called  $\varphi$ , and the perturbed one, called  $\varphi'$ . We stretch the reference signal from  
 87 a factor  $\epsilon$  and then compute the correlation coefficient between the stretched reference signal  
 88 and the perturbed one (Eq. 1) :

$$CC(\epsilon) = \frac{\int_{t_1}^{t_2} \varphi[t(1 + \epsilon)]\varphi'[t]dt}{\sqrt{\int_{t_1}^{t_2} \varphi^2[t(1 + \epsilon)]dt \int_{t_1}^{t_2} \varphi'^2[t]dt}} . \quad (1)$$

89 This operation is repeated for various values of  $\epsilon$ . The  $\epsilon$  value which maximizes  $CC$  is named  
 90  $\theta$ , and corresponds to the apparent relative velocity change. We also define  $Kd = 1 - CC(\theta)$ ,

91 which corresponds to the residual decorrelation between the two waveforms, after correction of  
 92 the phase change. The study of  $Kd$  constitutes the Coda Wave Decorrelation [Cowan et al., 2002,  
 93 Larose et al., 2010] (in fluids filled with a suspension of moving scatterers, Diffuse Acoustic Wave  
 94 Spectroscopy gives  $\theta = 0$  and  $Kd \neq 0$ ). It is important to note that  $Kd$  and  $\theta$  are computed  
 95 for a given time window  $[t_1, t_2]$  in the coda. The position of this window yields information  
 96 about the region of the medium being probed. Indeed, the later we look in the signal, the larger  
 97 and deeper is the area in which waves have traveled. If the changes were homogeneous in the  
 98 medium,  $\theta$  and  $Kd$  would be the same for any window position.  $\theta$ , the apparent velocity change,  
 99 would then become the actual homogeneous relative velocity change taking place in the medium.  
 100 This is obviously not the case here.

101 We show in Fig. 3 the evolution of  $Kd$  and  $\theta$  versus the water front elevation, for the  
 102 observation window  $[0.4 \text{ ms}, 0.8 \text{ ms}]$ . Error bars in Fig. 3 correspond to the error on  $\theta$  induced  
 103 in the signal processing (Eq. 1) by the presence of decorrelation. We used for its calculation  
 104 the formula given by [Weaver et al., 2011] which shows that this error, beside increasing with  
 105  $Kd$ , also depends on the time-window length and position, along with other parameters such as  
 106 central frequency and bandwidth.

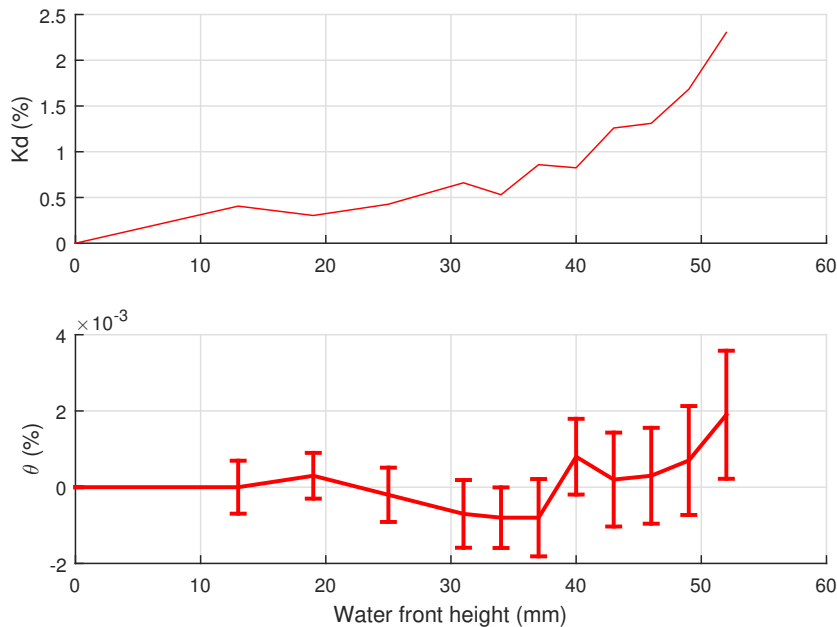


Figure 3: Evolution of stretching observables with water progression in sand.

107 It is clear in Fig. 3 that  $Kd$  is increasing with water elevation. It also increases with the  
 108 observation time in the coda (not shown here), which is coherent since the later we look in  
 109 the coda, the deeper waves have propagated and the longer they have interacted with changes.  
 110 This proves that  $Kd$  is sensitive to water presence.  $\theta$  results are however more difficult to

111 interpret. Although we can observe variations with water level, they are not much higher than  
 112 the estimated error bars, which suggests that changes in the waveform are dominating those in  
 113 phase. In other words, in the case of water imbibition in sand, structural changes occurring at  
 114 the grain scale are more important than mechanical changes (effective velocity) occurring in the  
 115 mesoscopic effective medium. CWD hence is a better indicator of water presence in sand than  
 116 CWI. In the following sections, we confront this observation with other experiments results,  
 117 as water imbibition in concrete, snow melt infiltration in rocky glaciers, or lava migration in  
 118 volcanoes.

### 119 **3 Monitoring of water imbibition in concrete**

120 In the litterature, experimental works [Garnier et al., 2013, Abraham et al., 2012, Popovics, 2005,  
 121 Balayssac et al., 2012] show variations of ballistic ultrasonic waves velocities of 10 % when homo-  
 122 geneous water saturation varies from 35 % to 100 %. In the case of a non homogeneous change,  
 123 for which the medium perturbation would be smaller, the higher sensitivity of coda waves could  
 124 be an important asset to detect or locate the changes.

125 We here present the results of an experiment originally designed to image a water content  
 126 gradient, in a concrete slab submitted to capillary imbibition. Concrete characteristics are  
 127 reported in Table 1 and a schematic description of the experimental setup is given in Fig. 4.

|                     |                         |
|---------------------|-------------------------|
| Max. aggregate size | 14 mm                   |
| Water/cement ratio  | 0.8                     |
| Density             | 2250 kg m <sup>-3</sup> |
| Open porosity       | 18 %                    |

Table 1: Concrete characteristics.

128 Before the experiment, the concrete slab (600 × 260 × 150 mm) is partially dried during several  
 129 weeks and is then water tight sealed, to ensure a uniform sample without initial water content  
 130 gradient. The initial (homogeneous) saturation is about 35 %, which places us in the saturation  
 131 regime marked by an increase of ballistic waves velocity, according to [Abraham et al., 2012].  
 132 At the beginning of the experiment, the inferior side is submerged in water. Supports have a  
 133 very limited contact area to limit acoustical transfer in other solids. The fluid level above the  
 134 bottom of the slab is maintained constant to around 1 cm so the water pressure underneath the  
 135 sample is close to the air pressure just above the sample. The resulting pressure difference is  
 136 hence constant in time, about 1 mbar, which is considered sufficiently small to assume a non-  
 137 forced imbibition. In order to provoke a vertical phenomenon, lateral sides are covered with

138 waterproof resin while the top one is free. To monitor the water gradient's evolution, four  
 139 moisture sensors (thermo-hygrometric) are placed in the concrete sample at different heights,  
 140 several weeks before. The experiment is carried out in a climatic chamber maintained at constant  
 141 temperature. Ambient air temperature along with air humidity level are recorded.

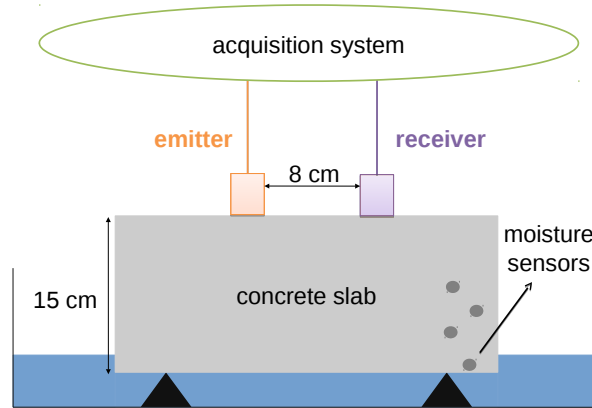


Figure 4: Experimental set-up.  
 Water imbibition in concrete is monitored using ultrasonic coda.

142 Ultrasonic emitters and receivers, glued on the top and one lateral side of the slab, retrieve  
 143 impulse responses in a 200 – 400 kHz frequency range. These responses are regularly measured in  
 144 time during the imbibition. For each sensor couple, the first signal measured after the beginning  
 145 of the imbibition is defined as the reference. We then use the stretching technique, described in  
 146 the previous section, to compare each of the following signals to this reference.

147 These comparisons gives us two observables: the apparent relative velocity change  $\theta$  and  
 148 the waveform decorrelation  $Kd$ , whose evolution during imbibition are given in Fig. 5, for one  
 149 source-receiver couple located on the top side of the block (see Fig. 4).

150 We first observe in Fig. 5 the difference of magnitude between the two observables.  $\theta$   
 151 presents indeed very weak variations. This particular point was not expected. According to  
 152 [Abraham et al., 2012], the (ballistic) relative velocity change in the fully saturated part of the  
 153 slab should be about 10%. Local variations, much smaller than this, have been detected us-  
 154 ing CWI [Zhang et al., 2016]. The fact that we are here not able to detect such an important  
 155 change is due to the high level of waveform decorrelation. Indeed, coda velocity is a property  
 156 of the effective medium, whereas decorrelation is related to micro-structural changes. Here,  
 157 these changes are too important to support the hypothesis of a continuously changing effective  
 158 medium. And comparing velocities during these changes has little meaning. In other words, the  
 159 conditions of CWI are not respected, particularly the hypothesis of path conservation. For the  
 160 velocity change to be properly defined in the material, the change should be at a scale much

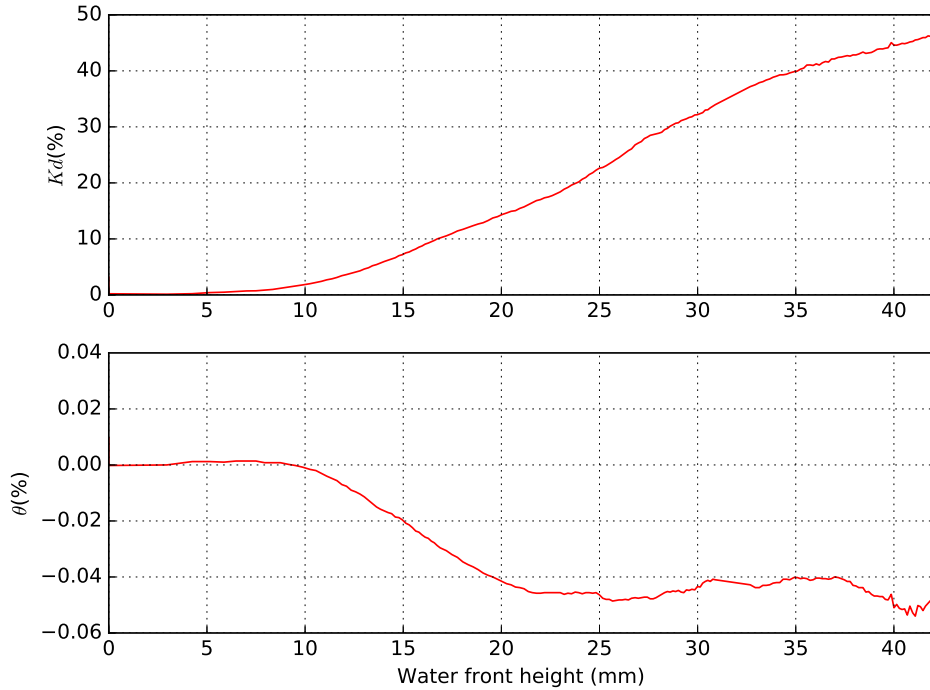


Figure 5: Evolution of stretching observables during water imbibition in concrete.

161 smaller than the wavelength.

162 As in previous section,  $Kd$  is hence found to be much more sensitive to water presence than  
 163  $\theta$ . In the following section, we attempt to use this observation to bring new interpretations in  
 164 other works, involving fluid in porous media, in a geophysical context.

## 165 4 Insights and perspectives from geophysical works

### 166 4.1 Rocky glaciers

167 As a field aiming to study the modifications of surface wave propagation related to external en-  
 168 vironmental changes, environmental seismology [Larose et al., 2015] may also be an interesting  
 169 tool for permafrost destabilization assessment. In this view, CWI and CWD are now used to  
 170 monitor physical evolutions of rocky glaciers. As the most prominent features in alpine per-  
 171 mafrost, and a common occurrence in arctic regions [Schoeneich et al., 2015], rocky glaciers are  
 172 tongue-shaped bodies of frozen debris matrices with interstitial ice [Arenson et al., 2002]. This  
 173 porous medium with important heterogeneities is seasonally subject to snow melt infiltration.  
 174 We here focus on the field work conducted on the Gugla rocky glacier site (Wallis, Switzerland),  
 175 where the first seismological monitoring of a rocky glacier takes place. Six seismic sensors record  
 176 permanent ambient noise data since Autumn 2015. Correlations between recordings of two sen-  
 177 sors located along a cross section of the rocky glacier, allow to retrieve the associated Green

178 function, which exhibits coda. Indeed, rocky glacier are heterogeneous media, thus causing mul-  
 179 tiple scattering at high frequencies (here from 10 to 14 Hz). Relative velocity changes occurring in  
 180 the medium can thus be measured, by applying the stretching method between a coda retrieved  
 181 in a reference period (corresponding to an initial stable state of the medium) to the coda from  
 182 the day of interest. The two observables (relative velocity change of the Rayleigh wave  $dV/V$   
 183 and decorrelation  $Kd$ ) have been linked to meteorological variables [Guillemot et al., ] (article  
 184 in preparation). Schematic representation of these observables variations are presented in Fig. 6.

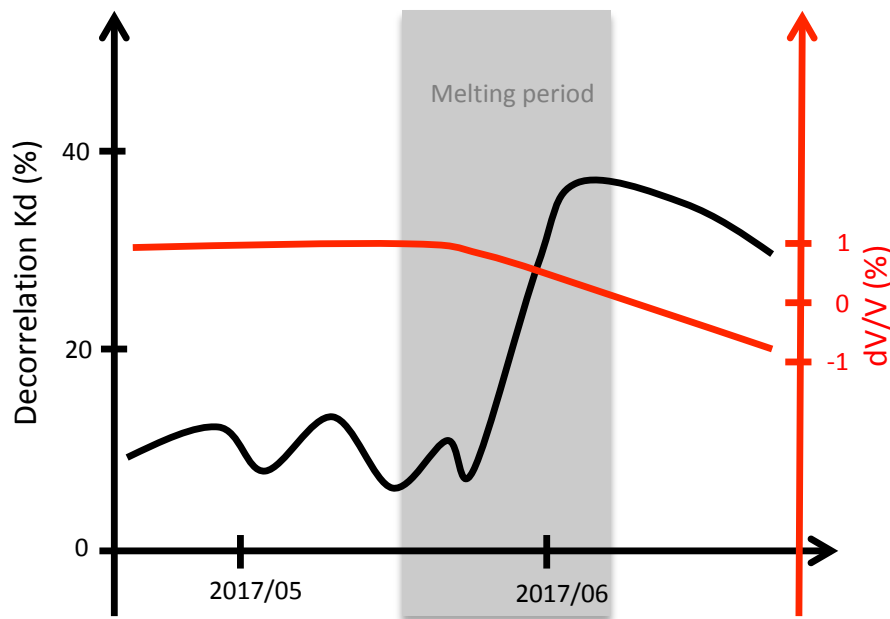


Figure 6: Schematic representation of  $Kd$  and  $\theta$ , measured in Gugla-Breithorn rock glacier (Switzerland) during a snow melting period, where melted snow is infiltrating through the porous structure. Curves interpreted from [Guillemot et al., ] (article in preparation).

185 We can observe a velocity drop during the melting period, and a simultaneous decorrelation  
 186 event. Whereas  $Kd$  seems to vary with the volume of water (rain and melted snow) infiltrating  
 187 in surface porous layers,  $dV/V$  variations exhibit better correlation with snow depth evolution  
 188 [Guillemot et al., ].

189 This study thus confirms the two findings presented in previous sections. First, decorrelation is  
 190 sensitive to pore filling, and can be an interesting indicator to monitor water content changes.  
 191 Secondly, velocity doesn't seem to be very sensitive to fluid infiltration. However in this case,  
 192  $dV/V$  is related to rigidity or density changes, and thus can be relevant as precursor of a global  
 193 destabilization of rocky glacier, due to melting effects (but is smaller than  $Kd$  in absolute value  
 194 and, thus, less sensitive).

## 195 4.2 Volcanoes

196 In the field of seismology, CWI and CWD have naturally been used to monitor volcanic areas,  
197 whose important heterogeneity makes coda-based methods attractive. We here focus on the  
198 work made by [Obermann et al., 2013] on the Piton de la Fournaise. This work is based on  
199 records made during six months around two eruptions, and proposes 2D-mapping of the velocity  
200 change and the cross section density change. To do this imagery, they define a direct problem  
201 involving sensitivity kernels, to link the apparent velocity change  $\theta$ , measured by stretching, to  
202 the actual velocity change distribution. The same goes with the cross section density of changes,  
203 which is related to  $Kd$ , and quantifies the micro-structural changes occurring at the scatterer  
204 scale. These maps are made at different steps of the eruptions.

205 In this earlier work, velocity changes are supposed to be generated by soil fracturation and  
206 inflation due to movements of the pressurized fluid (magma) underneath. The cross section  
207 change is interpreted as cracks opening and development, due to the same pressure fluid, and is  
208 found to be a more sensitive indicator.

209 Although this work is well interpreted, ours permits to bring confirmations to certain hypothesis.  
210 The first one is that the velocity is weakly impacted by fluid presence but mostly by microfrac-  
211 turation (at sizes much smaller than the seismic wavelength). The second one is that decor-  
212 relation is more sensitive, and actually more spatially resolved, than relative velocity changes.  
213 Third, decorrelation – and cross section – could be due, not only to the crack opening, but also  
214 to fluid injection.

## 215 5 Conclusion

216 In this article, two laboratory experiments have been presented, in which water ascends either in  
217 a sand or a concrete medium. For each experiment, ultrasonic waves are emitted and recorded  
218 from the sample surface. CWI and CWD methods are applied to the measured coda signals,  
219 hence giving phase shift and decorrelation values for various water levels.

220 While we expected both these observables to be sensitive to water elevation, these experiments  
221 have shown that water impacts more importantly the decorrelation. The phase shift, correspond-  
222 ing to the apparent relative velocity change, hardly emerges from noise or has very low values.  
223 This observation contrasts with results found in literature for ballistic waves. Our experiments  
224 hence show that the velocity change induced by water on ballistic waves is no longer visible when  
225 we decrease the wavelength, because of the impact of water on the scatterers (heterogeneities).

226 When looking at the scattered waves, changes in the medium microstructure dominate those in  
227 the effective medium.

228 We have then showed that this simple observation could be retrieved in geophysical field  
229 studies, such as rocky glacier under snow melt infiltration, and pre-eruptive volcano. In those  
230 studies, this new considerations bring some light on the initial interpretations, and allow better  
231 comprehension of the problems.

## 232 Acknowledgments

233 The first author acknowledge PhD grant funding from IFSTTAR. This work is partially funded  
234 by the "ANR ENDE" and "IDEX - Univ. Grenoble Alpes" projects. We also thank J.B. Legland,  
235 G. Villain, and O. Durand for their help on the concrete experiment.

## 236 References

- 237 [Abraham et al., 2012] Abraham, O., Piwakowski, B., Villain, G., & Durand, O. (2012). Non-  
238 contact, automated surface wave measurements for the mechanical characterisation of con-  
239 crete. *Construction and Building Materials*, 37, 904–915.
- 240 [Archie, 1942] Archie, G. (1942). The Electrical Resistivity Log as an Aid in Determining Some  
241 Reservoir Characteristics. *Transactions of the AIME*, 146(01), 54–62.
- 242 [Arenson et al., 2002] Arenson, L., Hoelzle, M., & Springman, S. (2002). Borehole deformation  
243 measurements and internal structure of some rock glaciers in Switzerland. *Permafrost and*  
244 *Periglacial Processes*, 13(2), 117–135.
- 245 [Balayssac et al., 2012] Balayssac, J. P., Laurens, S., Arliguie, G., Breyse, D., Garnier, V.,  
246 Dérobert, X., & Piwakowski, B. (2012). Description of the general outlines of the French  
247 project SENSO - Quality assessment and limits of different NDT methods. *Construction and*  
248 *Building Materials*, 35, 131–138.
- 249 [Barker & Moore, 1998] Barker, R. & Moore, J. (1998). The application of time-lapse electrical  
250 tomography in groundwater studies. *The Leading Edge*, 17(10), 1454–1458.
- 251 [Benson, 1991] Benson, R. C. (1991). Remote Sensing and geophysical methods for evalua-  
252 tion of subsurface conditions. In D. M. Nielsen (Ed.), *Practical Handbook of Environmental*  
253 *Site Characterization and Ground-Water Monitoring* (pp. 143–194). Lewis Publishers Inc.,  
254 Chelsea, Michigan.

255 [Brennguier et al., 2008] Brennguier, F., Campillo, M., Hadziioannou, C., Shapiro, N. M., Nadeau,  
256 R. M., & Larose, E. (2008). Postseismic relaxation along the San Andreas fault at Parkfield  
257 from continuous seismological observations. *Science*, 321(5895), 1478–1481.

258 [Cowan et al., 2002] Cowan, M. L., Jones, I. P., Page, J. H., & Weitz, D. A. (2002). Diffusing  
259 acoustic wave spectroscopy. *Physical Review E - Statistical, Nonlinear, and Soft Matter*  
260 *Physics*, 65(6), 1–23.

261 [Garnier et al., 2013] Garnier, V., Piwakowski, B., Abraham, O., Villain, G., Payan, C., &  
262 Chaix, J. F. (2013). Acoustic techniques for concrete evaluation: Improvements, comparisons  
263 and consistency. *Construction and Building Materials*, 43, 598–613.

264 [Grêt et al., 2006] Grêt, A., Snieder, R., & Scales, J. (2006). Time-lapse monitoring of rock  
265 properties with coda wave interferometry. *Journal of Geophysical Research: Solid Earth*,  
266 111(3), 1–11.

267 [Guillemot et al., ] Guillemot, A., Baillet, L., Helmstetter, A., Larose, É., & Mayoraz, R. Seis-  
268 mic monitoring of the Gugla-Breithorn rock glacier (Switzerland) – In preparation.

269 [Jia, 2004] Jia, X. (2004). Codalike multiple scattering of elastic waves in dense granular media.  
270 *Physical Review Letters*, 93(15), 8–11.

271 [Jia et al., 2009] Jia, X. P., Laurent, J., Khidas, Y., & Langlois, V. (2009). Sound scattering in  
272 dense granular media. *Chinese Science Bulletin*, 54(23), 4327–4336.

273 [Konstantaki et al., 2013] Konstantaki, L., Carpentier, S., Garofalo, F., Bergamo, P., & Socco,  
274 L. (2013). Determining hydrological and soil mechanical parameters from multichannel  
275 surface-wave analysis across the Alpine Fault at Inchbonnie, New Zealand. *Near Surface*  
276 *Geophysics*, 11(1983), 435–448.

277 [Larose et al., 2015] Larose, E., Carrière, S., Voisin, C., Bottelin, P., Baillet, L., Guéguen, P.,  
278 Walter, F., Jongmans, D., Guillier, B., Garambois, S., Gimbert, F., & Massey, C. (2015).  
279 Environmental seismology: What can we learn on earth surface processes with ambient noise?  
280 *Journal of Applied Geophysics*, 116, 62–74.

281 [Larose & Hall, 2009] Larose, E. & Hall, S. (2009). Monitoring stress related velocity variation  
282 in concrete with a 2.10<sup>-5</sup> relative resolution using diffuse ultrasound. *The Journal of the*  
283 *Acoustical Society of America*, 125(4), 1853–1856.

284 [Larose et al., 2010] Larose, E., Planes, T., Rossetto, V., & Margerin, L. (2010). Locating a  
285 small change in a multiple scattering environment. *Applied Physics Letters*, 96(20), 204101.

286 [Lobkis & Weaver, 2003] Lobkis, O. I. & Weaver, R. L. (2003). Coda-Wave Interferometry in  
287 Finite Solids: Recovery of P-to-S Conversion Rates in an Elastodynamic Billiard. *Physical  
288 Review Letters*, 90(25), 254302.

289 [Lu & Sabatier, 2009] Lu, Z. & Sabatier, J. M. (2009). Effects of Soil Water Potential and  
290 Moisture Content on Sound Speed. *Soil Science Society of America Journal*, 73(5), 1614.

291 [Obermann et al., 2013] Obermann, A., Planès, T., Larose, E., & Campillo, M. (2013). Imaging  
292 preeruptive and coeruptive structural and mechanical changes of a volcano with ambient  
293 seismic noise. *Journal of Geophysical Research: Solid Earth*, 118(12), 6285–6294.

294 [Popovics, 2005] Popovics, S. (2005). Effects of uneven moisture distribution on the strength of  
295 and wave velocity in concrete. *Ultrasonics*, 43(6), 429–434.

296 [Schoeneich et al., 2015] Schoeneich, P., Bodin, X., Echelard, T., Kaufmann, V., Kellerer-  
297 Pirklbauer, A., Krysiecki, J. M., & Lieb, G. K. (2015). Velocity Changes of Rock Glaciers and  
298 Induced Hazards. In *Engineering Geology for Society and Territory - Volume 1* (pp. 223–227).  
299 Cham: Springer International Publishing.

300 [Sens-Schönfelder & Wegler, 2006] Sens-Schönfelder, C. & Wegler, U. (2006). Passive image  
301 interferometry and seasonal variations of seismic velocities at Merapi Volcano, Indonesia.  
302 *Geophysical Research Letters*, 33(21), 1–5.

303 [Snieder, 2006] Snieder, R. (2006). The theory of coda wave interferometry. *Pure and Applied  
304 Geophysics*, 163(2-3), 455–473.

305 [Snieder et al., 2002] Snieder, R., Grêt, A., Douma, H., & Scales, J. (2002). Coda wave interfer-  
306 ometry for estimating nonlinear behavior in seismic velocity. *Science*, 295(5563), 2253–2255.

307 [Villain et al., 2012] Villain, G., Sbartaï, Z. M., Dérobert, X., Garnier, V., & Balayssac, J.-  
308 P. (2012). Durability diagnosis of a concrete structure in a tidal zone by combining NDT  
309 methods: Laboratory tests and case study. *Construction and Building Materials*, 37, 893–  
310 903.

311 [Weaver et al., 2011] Weaver, R. L., Hadziioannou, C., Larose, E., & Campillo, M. (2011). On  
312 the precision of noise correlation interferometry. *Geophysical Journal International*, 185(3),  
313 1384–1392.

- 314 [Winkler & Nur, 1979] Winkler, K. & Nur, A. (1979). Pore fluids and seismic attenuation in  
315 rocks. *Geophysical Research Letters*, 6(1), 1–4.
- 316 [Zhang et al., 2012] Zhang, Y., Abraham, O., Grondin, F., Loukili, A., Tournat, V., Duff, A. L.,  
317 Lascoup, B., & Durand, O. (2012). Study of stress-induced velocity variation in concrete under  
318 direct tensile force and monitoring of the damage level by using thermally-compensated Coda  
319 Wave Interferometry. *Ultrasonics*, 52(8), 1038–1045.
- 320 [Zhang et al., 2018] Zhang, Y., Larose, E., Moreau, L., & D’Ozouville, G. (2018). Three-  
321 dimensional in-situ imaging of cracks in concrete using diffuse ultrasound. *Structural Health*  
322 *Monitoring*, 17(2), 279–284.
- 323 [Zhang et al., 2016] Zhang, Y., Planès, T., Larose, E., Obermann, A., Rospars, C., & Moreau,  
324 G. (2016). Diffuse ultrasound monitoring of stress and damage development on a 15-ton  
325 concrete beam. *The Journal of the Acoustical Society of America*, 139(4), 1691–1701.